

# **A General Method for Fatigue Analysis of Vertical Axis Wind Turbine Blades**

**Paul S. Veers**

Prepared by  
Sandia National Laboratories  
Albuquerque, New Mexico 87185 and Livermore, California 94550  
for the United States Department of Energy  
under Contract DE-AC04-76DP00789



Issued by Sandia National Laboratories, operated for the United States Department of Energy by Sandia Corporation.

**NOTICE:** This report was prepared as an account of work sponsored by an agency of the United States Government. Neither the United States Government nor any agency thereof, nor any of their employees, nor any of their contractors, subcontractors, or their employees, makes any warranty, express or implied, or assumes any legal liability or responsibility for the accuracy, completeness, or usefulness of any information, apparatus, product, or process disclosed, or represents that its use would not infringe privately owned rights. Reference herein to any specific commercial product, process, or service by trade name, trademark, manufacturer, or otherwise, does not necessarily constitute or imply its endorsement, recommendation, or favoring by the United States Government, any agency thereof or any of their contractors or subcontractors. The views and opinions expressed herein do not necessarily state or reflect those of the United States Government, any agency thereof or any of their contractors or subcontractors.

Printed in the United States of America  
Available from  
National Technical Information Service  
U.S. Department of Commerce  
5285 Port Royal Road  
Springfield, VA 22161

NTIS price codes  
Printed copy: A02  
Microfiche copy: A01

# A General Method for Fatigue Analysis of Vertical Axis Wind Turbine Blades\*

Paul S. Veers  
Applied Mechanics Division IV 1524  
Sandia National Laboratories  
Albuquerque, NM 87185

## Abstract

The fatigue life of wind turbine blades that are exposed to the random loading environment of atmospheric winds is described with random data analysis procedures. The incident wind speed and the stresses caused by these winds are expressed in terms of probability density functions, while the fatigue life vs stress level relationship is treated deterministically. This approach uses a "damage density function" to express fatigue damage as a function of wind speed. By examining the constraints on the variables in the damage density expression, some generalizations of the wind turbine fatigue problem are obtained. The area under the damage density function is inversely related to total fatigue life. Therefore, an increase in fatigue life caused by restricted operation in certain wind regimes is readily visualized. An "on parameter", which is the percentage of total time at each wind speed that the turbine actually operates, is introduced for this purpose. An example calculation is presented using data acquired from the DOE 100-kW turbine program.

---

\*This work was performed at Sandia National Laboratories and was supported by the US Department of Energy under Contract Number DE-AC04-76DP00789.

## **Acknowledgments**

The calculations required to produce the figures in this paper would not have been possible without the work of Jerry McNerney and Tim Leonard in developing the AUTOSYM computer simulation. The efforts of Nolan Clark and Ron Davis in collecting data for the DOE 100-kW turbine at the USDA station in Bushland, TX are greatly appreciated.

# A General Method for Fatigue Analysis of Vertical Axis Wind Turbine Blades

## Introduction

The fatigue life of wind turbine blades is a necessary ingredient in the estimate of the cost effectiveness of a wind turbine system. Ideally, rotor control parameters (such as the cutin and cutout wind speeds) should be selected to maximize both turbine life and rate of energy capture. However, energy capture (on a yearly basis) and blade fatigue life are conflicting quantities that require trade offs to determine the most suitable operating mode for a given wind system. The goal of this fatigue analysis is to define techniques that help to clarify the balance between rotor life expectancy and the rate of energy production.

Because the turbine operates in a random-loading environment, a statistical approach to defining the operating stresses is used. Reference 1 describes the method used to produce an estimate of blade life based upon descriptions of the cyclic stresses and wind speeds in terms of probability density functions (pdf). By using Miner's cumulative damage rule, the damage produced by the stress cycles at each stress amplitude within the pdf are integrated to estimate the blade life. However, Reference 1 does not include the effects of the control system. Since evaluating the control system that turns the turbine on and off is a goal of the fatigue analysis, it is important to know which wind speeds cause the bulk of the fatigue damage. A damage density function (ddf) that plots damage as a function of wind speed is introduced for this purpose. In a similar way, the amount of energy available at each wind speed is expressed in terms of an energy density function (edf). Both the maximum energy and maximum damage are accumulated if the wind turbine is operated (on) at all times. The life expectancy of the rotor is extended by incorporating a high-wind cutout in the turbine control algorithm. The effect of this cutout algorithm is expressed by plotting an "on parameter" that shows the fraction of the total available time at each wind speed actually operated by the turbine. In general, the on parameter is less than the unity between cutin and cutout, and above zero elsewhere because of the wind speed averaging times associated with the control algorithms.

The operating edf and ddf are found by multiplying the maximum edf and ddf by the on parameter. The area under the edf is related to the annual energy production and the area under the ddf is related to the inverse of the blade fatigue life.

This approach allows the analyst to visualize the effect of changing algorithm parameters on the fatigue life and energy production rate of the turbine. The ideal algorithm is one that removes as much area as possible from the ddf, thus increasing rotor life expectancy without taking area from the edf, thus maximizing the annual energy production. It is important to remember that the fatigue life and energy capture of a turbine are inseparable components of a cost of energy estimate.

The damage accumulated while the turbine is parked and during start-stop cycles is not included in this analysis procedure. Data collected during testing of several Darrieus Vertical Axis Wind Turbine (VAWT) systems support the assumption that these events have negligible effect on blade fatigue life. This is not necessarily a universal truth, but should be checked for each turbine individually.

## Damage Density and Energy Density

In order to examine the effects of the operating parameters on the rotor fatigue life, it is convenient to know which wind speeds are responsible for the most damage. This can be visualized by plotting the damage as a function of wind speed in terms of a ddf. The ddf is derived in Appendix A. Although the stress levels (and hence the damage rate) continue to rise as wind speed increases, the amount of wind available at higher wind speeds decreases. The net result is that the ddf goes to zero as wind speeds continue to rise. The area under the ddf is the inverse of the blade life expectancy. The ddf for the blade to tower joint of the DOE 100-kW turbine at the Bushland, TX site is

shown in Figure 1. This ddf is calculated as if the turbine operates at all times. The calculation of this ddf and the data used to produce it are included in Appendix B.

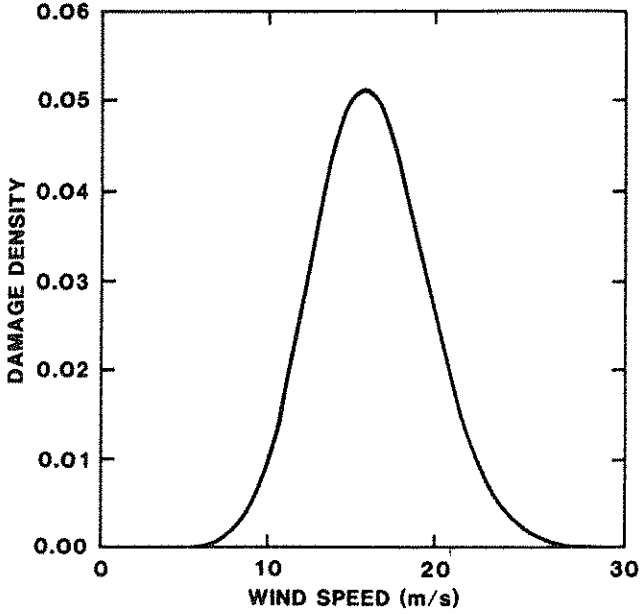


Figure 1. Damage Density Function (ddf) for the Welded Blade Joint of the DOE 100-kW Turbine at Bushland, TX

To summarize the results of Appendices A and B, if the pdf of wind is Rayleigh,

$$P_v(V) = \frac{\pi V}{2\bar{V}^2} \exp\left(\frac{-\pi V^2}{4\bar{V}^2}\right) \quad (1)$$

the standard deviation of the stress varies linearly with wind speed,

$$\sigma(V) = mV \quad (2)$$

and the number of cycles to failure can be described by a power function of the standard deviation of the stresses,

$$N(\sigma) = K\sigma^b \quad (3)$$

then the maximum ddf, assuming that the turbine is always operating, will be as shown in Appendix B, Eq (B2)

$$d_v(V) = \frac{\pi m^{-b}}{2\bar{V}^2 K} V^{(1-b)} \exp\left(\frac{-\pi V^2}{4\bar{V}^2}\right) \quad (4)$$

The relationships described by Eqs (1), (2), and (3) have been found to be very accurate for the DOE 100-kW machines and are useful approximations.

The general shape of the maximum ddf is as shown in Figure 1. The peak of the ddf is at a wind speed of

$$V_{\text{peak}} = \bar{V} \sqrt{\frac{2}{\pi}(1-b)} \quad (5)$$

Observe that the peak of the maximum ddf is a function only of the average wind speed ( $\bar{V}$ ) and the fatigue life exponent ( $b$ ). (The fatigue life exponent is the slope of the RMS stress vs cycles to failure curve when plotted log-log.) At the high-cycle end of the fatigue life curve, the slope is, in general, quite flat; typical values of the exponent ( $b$ ) are between  $-5$  and  $-12$ . This puts the peak of the ddf between 2 and 3 times the annual average wind speed. As a result of the flat nature of the fatigue-life curve at high cycles, small changes in the operating stress level or in the fatigue-life curve produce large changes in the life estimate. Therefore, a reliable fatigue-life estimate requires an accurate description of the operating stresses and a statistical description of the fatigue-life characteristics. A family of fatigue-life curves for various confidence levels should be produced. Then a fatigue-life estimate can be described based upon a specified confidence level. Unfortunately, defining the statistics of the fatigue-life curve requires a large number of tests of the blade components.

The energy-capture characteristics of a turbine in a particular site are often described using an edf analogous to the ddf. The maximum edf is the product of the wind speed pdf and the power curve. A convenient way to visualize the trade off between fatigue life and energy capture is to plot both the edf and the ddf on the same wind speed axis. Figure 2 is a plot that includes the edf and two extreme cases of the ddf; the first with a high slope on the fatigue-life curve ( $b = -5$ ) that results in a peak at  $2\bar{V}$ , and the second with a low slope on the fatigue curve ( $b = -12$ ) that produces a peak at  $3\bar{V}$ . The peak of the maximum edf will typically be at about 1.5 times the average wind speed. Note that the bulk of the damage is usually accumulated at higher wind speeds than the bulk of the available energy. This makes it possible to obtain a significant extension in the blade fatigue life without sacrificing a great deal of the available energy by shutting down the turbine at the appropriate time.

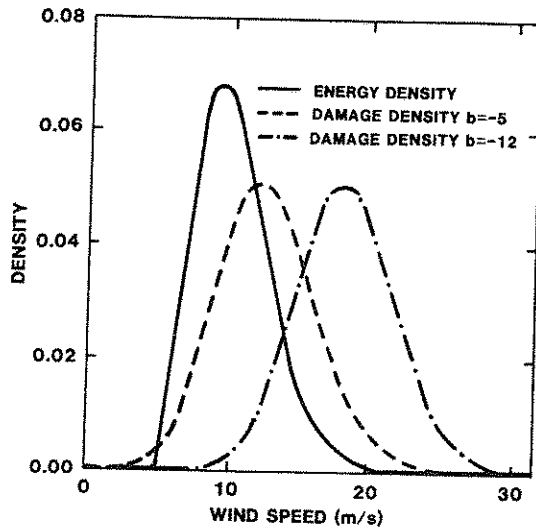


Figure 2. Energy Density Function (edf) With Two Limiting Cases of the Damage Density Function (ddf)

## Control Algorithm Effects

The purpose of the cutout algorithm is therefore to balance the extension of fatigue life with the reduction in the annual energy capture, both of which result from shutting down the turbine in high winds. To visualize the effect of the control algorithm on the operation of the turbine, an "on parameter" is defined which shows the fraction of the total available time at each wind speed that a turbine operates. The on parameter for a given wind speed is zero if the turbine never operates at that wind speed and 1 if the turbine always operates when the winds are at the given wind speed. Figure 3 plots the on parameter for several cutout wind speeds. This on parameter was calculated by a Sandia computer simulation called AUTOSYM<sup>2</sup> using wind data collected at Bushland, TX. The algorithm shuts the turbine off when a 2-s average of the wind speed exceeds the cutout and will not restart until 15 min after any cutout wind speed exceedence. This is by no means an optimum algorithm but is included as an example. The dashed line would be the on parameter for a turbine that is always on. The on parameter never reaches 1 because the winds may be inside the operating range while the turbine is in the middle of a start-up averaging period or in a 15-min shutdown after a high wind cutout. As expected, operation in winds above cutout is practically eliminated. But a by-product of this algorithm (or any algorithm) is a considerable reduction in operating time in winds well below cutout.

The actual, or operating, edf and ddf are obtained by multiplying the maximum edf and pdf by the on

parameter. The ddf's in Figure 4 are calculated by combining the on parameters in Figure 3 with the damage density in Figure 1. Since the area under the ddf is the inverse of the blade fatigue life, the reduced areas under the ddf's associated with lower cutout wind speeds indicate increased blade life. Similarly, the family of edf's for different cutout wind speeds plotted in Figure 5 show how the annual energy capture is affected by the cutout algorithm. Note that, with a 20.1 m/s (45 mph) cutout, almost all of the available energy is captured while a substantial fraction of the fatigue damage is still eliminated. Table 1 lists the blade fatigue life expectancy and annual energy capture associated with edf's and ddf's for the blade-to-tower joints on the DOE 100-kW turbine at Bushland, TX, shown in Figures 5 and 4, respectively.

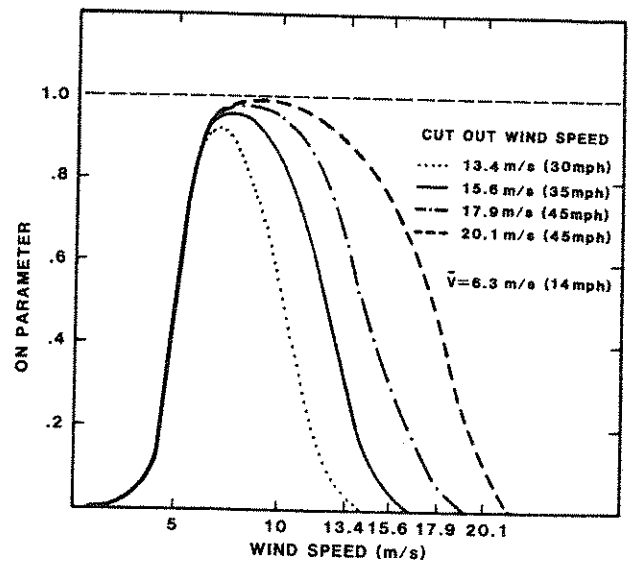


Figure 3. On Parameters for Several Values of Cutout Wind Speed for the DOE 100-kW Turbine at Bushland, TX

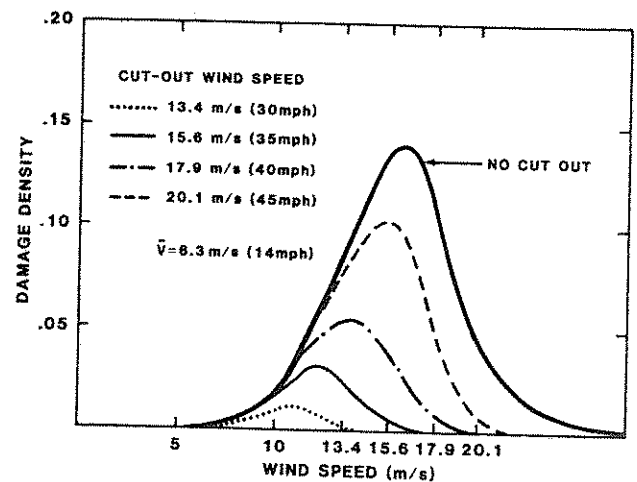


Figure 4. Damage Density Functions for Several Values of Cutout Wind Speed

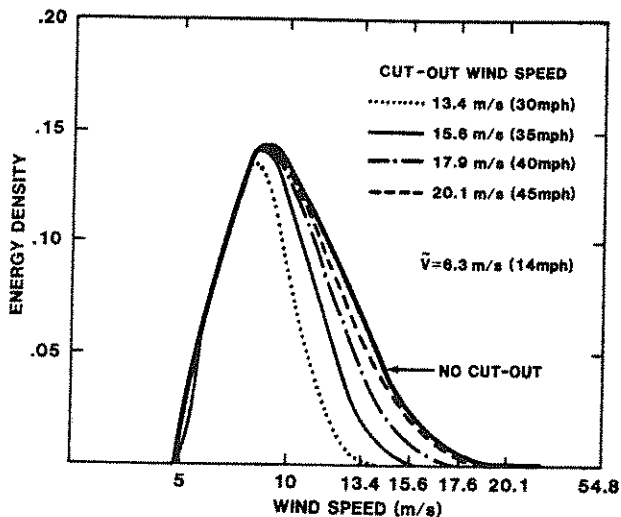


Figure 5. Energy Density Functions for Several Values of Cutout Wind Speed

Table 1. Effects of Cutout Wind Speed

Cutout Wind Speed (m/s)	Cutout Wind Speed (mph)	Annual Energy (fraction of maximum)*	Expected Joint Life (multiple of minimum)*
13.4	30	0.49	22.0
15.6	35	0.69	7.0
17.9	40	0.83	3.1
20.1	45	0.92	1.6
22.4	50	0.95	1.2

\*Maximum energy and minimum joint life are calculated based upon a turbine that never shuts down in high winds. For the DOE 100-kW turbine at Bushland ( $\bar{V} = 6.3$  m/s; 14 mph) the maximum energy is 200 000 kWh and the minimum joint life is 2.8 yrs.

## Statistical Considerations

The data presented here is used to produce an estimate of the mean component fatigue life. There

are two very important points that must be made: first, this is the mean (or 50%) confidence level of the fatigue life; second, it is the fatigue life of a single component (such as one joint) and not the entire rotor. If there is a P percent confidence that a component will not fail in T years and there are n components in the rotor, then the confidence that the rotor will not fail in T yr is

$$P_{\text{rotor}} = P^n \quad (6)$$

For example, if there is a 50% confidence that one joint on the Bushland turbine will not fail for 5 yr and there are four similar joints on the rotor experiencing the same stress levels, there is only a 6.25% confidence that the rotor will not fail in 5 yr. In order to obtain a 50% confidence or mean rotor life, the fatigue life of each joint would have to be known at an 84% confidence level. Producing an RMS-N curve at a given confidence level requires repeated tests at each stress level. Reference 3 outlines a procedure for evaluating the fatigue life curve at a given confidence level.

## Summary

By creating maximum damage and energy density functions, the lower bound on fatigue life and the upper bound on annual energy production are defined.

Figure 2 indicates that the bulk of the energy and the bulk of the damage will usually lie in different wind speed regimes. Therefore, a good cutout algorithm can reduce the damage significantly without crippling the system by overly restricting the annual energy production. The cutout algorithm is characterized by the on parameter that shows the fraction of the total available time at each wind speed the turbine actually operates. The actual ddf and edf are the product of the on parameter and the maximum ddf and edf. The expected time to failure is the inverse of the area under the actual ddf and the annual energy production is the area under the actual edf. The use of these density functions should aid the analyst in visualizing the fatigue life/energy capture trade-off.

## Bibliography

Broch, J. T., "Peak-Distribution Effects in Random-Load Fatigue," from *Effects of Environment and Complex Load History on Fatigue Life*, ASTM STP 462, 1968, pp 104-126.

Brown, G. W. and Ikegami, R., "The Fatigue of Aluminum Alloys Subjected to Random Loading," SESA Spring Meeting, Huntsville, AL, May 1970.

Miner, M. A., "Cumulative Damage in Fatigue," *ASME Journal of Applied Mechanics*, 1945.

Schijve, J., "Effects of Load Sequence on Crack Propagation Under Random and Program Loading," *Engineering Fracture Mechanics*, Vol 5, Pergamon Press, 1973, pp 267-280.

## References

<sup>1</sup>Veers, P. S., "Blade Fatigue Life Assessment With Application to VAWTS," *ASME Journal of Solar Energy Engineering*, Vol 104, May 1982.

<sup>2</sup>McNerney, G. M., *Vertical Axis Wind Turbine Control Strategy*, SAND81-1156 (Albuquerque, NM: Sandia National Laboratories, August 1981).

<sup>3</sup>Weibull, W., *Fatigue Testing and Analysis of Results* (Oxford: Pergamon Press, 1961).

<sup>4</sup>Akins, R. E., *Performance Evaluation of Wind Energy Conversion Systems Using the Method of Bins-Current Status*, SAND77-1375 (Albuquerque, NM: Sandia Laboratories, 1978).

<sup>5</sup>Akins, R. E., "Method-of-Bins Update," *Proceedings of the Wind Energy Expo '82*, Amarillo, TX, October 24-27, 1982.



## APPENDIX A

### Derivation of the Damage Density Function

Even though wind turbine blades have the cyclic loads caused by rotating through upwind and downwind orientations producing what could be expected to be deterministic loads, the turbulence in the wind causes the blade stresses to be stochastic rather than deterministic. There is evidence<sup>1</sup> that the distribution of cyclic stress amplitudes at any given wind speed follows the distribution of peak values of a Gaussian narrow band random process: namely, a Rayleigh distribution. This conditional probability density function (pdf) is

$$P_{s|v}(S,V) = \frac{S}{\sigma(V)^2} \exp\left(\frac{-S^2}{2\sigma(V)^2}\right) \quad (\text{A1})$$

where

S = stress amplitude  
V = wind speed  
 $\sigma(V)$  = standard deviation of the stress signal (written here as a function of wind speed)

In many cases,  $\sigma(V)$  may be a linear function of wind speed as it is for the DOE 100-kW rotor (Appendix B).

$$\sigma(V) = mV \quad (\text{A2})$$

The pdf for the stress amplitudes can be found from the joint pdf of stress amplitude and wind speed. The joint pdf is the product of the conditional pdf and the wind speed pdf. If the wind pdf is Rayleigh,

$$P_{s,v}(S,V) = \frac{S}{\sigma(V)^2} \exp\left(\frac{-S^2}{2\sigma(V)^2}\right) \quad (\text{A3})$$

the joint pdf of stress and wind speed will be

$$P_{s,v}(S,V) = \frac{S}{\sigma^2} \exp\left(\frac{-S^2}{2\sigma^2}\right) \frac{\pi V}{2\bar{V}^2} \exp\left(\frac{-\pi V^2}{4\bar{V}^2}\right) \quad (\text{A4})$$

The pdf of stress is the integral over all wind speeds of the joint pdf.

$$P_s(S) = \int_0^\infty P_{s,v}(S,V) dV \quad (\text{A5})$$

Substituting (A4) into (A5) and evaluating the integral yields

$$P_s(S) = CK_0(k\sqrt{R}) \quad (\text{A6})$$

where

$$C = \pi S / 2\bar{V}^2 m^2$$

$$k^2 = 2S^2 / m^2$$

$$R = \pi / 4\bar{V}^2$$

$\bar{V}$  = annual average wind speed

$K_0(\ )$  = modified Hankel function of order 0

Plots of the stress pdf of the DOE 100-kW rotor for three annual average wind speeds are shown in Figure A1.

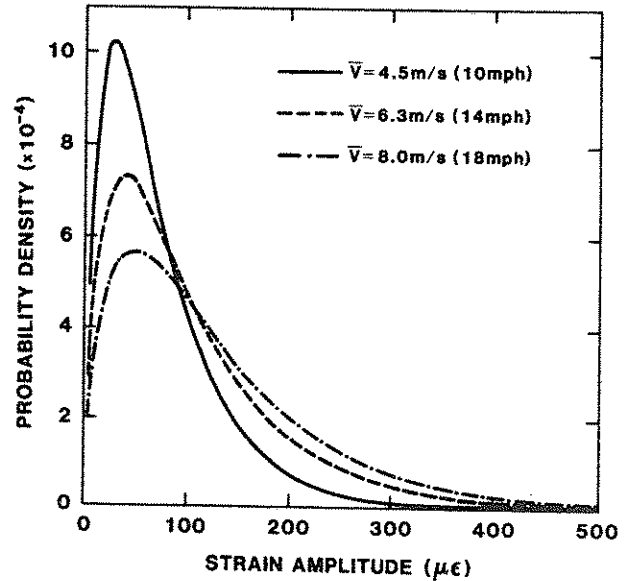


**Figure A1.** Probability Density Functions of the Vibratory Strain Amplitudes for the Welded Joint of the DOE 100-kW VAWT for Three Different Annual Average Wind Speeds

The total fatigue damage is the sum of the damage done by each stress amplitude. The damage is calculated by dividing the number of cycles at each stress level (described by  $P_s(S)$  times the total number of cycles) by the number of cycles to failure at each stress level. When the sum is equal to one, the total number of cycles equals the number of cycles to failure.

$$1 = \int_0^{\infty} \frac{n_f P_s(S)}{N(S)} dS \quad (A7)$$

where

$n_f$  = total cycles to failure (including all levels)  
 $N(S)$  = number of cycles to failure at the stress amplitude  $S$

The time to failure is the number of cycles to failure divided by the cyclic frequency. The estimated time to failure, assuming the turbine is always operating, is given by

$$\frac{1}{T} = f \int_0^{\infty} \frac{P_s(S)}{N(S)} ds \quad (A8)$$

where

$T$  = estimated time to failure  
 $f$  = mean crossing rate

If, however, the fatigue life of the component is known as a function of the standard deviation of the stress rather than the stress amplitude, solving for the estimated time to failure is much simpler and avoids some of the inaccuracies of using Miner's Rule. Since the standard deviation of stress can be written as a

function of wind speed (as in Eq (A2)), and the number of cycles to failure is a function of the stress standard deviation, the number of cycles to failure can be written directly as a function of wind speed.

$$N(\sigma) = N(\sigma(V)) = N(V) \quad (A9)$$

The time to failure can be solved for by integrating all possible wind speeds, again assuming that the turbine is always operating.

$$\frac{1}{T} = \int_0^{\infty} f \frac{P_v(V)}{N(V)} dV \quad (A10)$$

The integrand of this expression is the damage density function (ddf).

$$d_v(V) = f \frac{P_v(V)}{N(V)} \quad (A11)$$

This is actually the maximum ddf because it represents the relative amounts of damage accumulated at each wind speed for a turbine that is always operating. Whenever the turbine operates less than full time, the magnitude of the ddf is reduced and the area under the ddf is also reduced. Eq (A10) shows that the time to failure is inversely related to the area under the ddf. Therefore, the increase in life expectancy caused by restricted operation can be visualized by examining the effect on the ddf. For example, if the turbine blade characterized by the ddf in Figure 1 were always operated in winds below 16 m/s (36 mph) and never above, the expected time to failure of the blade would be about twice that of the blade on a turbine that always operates.

## APPENDIX B

### Example Damage Density Function Calculation

The DOE 100-kW Vertical Axis Wind Turbines (VAWTs) have been operating in Rocky Flats, CO, Bushland, TX, and Martha's Vineyard, MA. As a concrete example of the fatigue analysis method described above, the field data collected at Bushland and the testing done on the DOE 100-kW system are presented here. The welded joint at the blade-to-tower connection was selected for this fatigue life estimate. To produce a maximum ddf for the turbine always operating, the component fatigue life, operating stress levels, and cyclic stress frequency must be characterized. The wind distribution used for this example is for the Bushland site which closely matches a Rayleigh distribution with a 6.3 m/s (14 mph) mean.

#### Fatigue Life Data

The testing was accomplished by mounting a specially designed test specimen on an electromagnetic shaker. The specimen was shaken at its first resonant frequency with a random narrow band input. The resulting cyclic stress amplitude distribution matches the operating conditional pdf of cyclic stress amplitude. This distribution is characterized by the RMS of the stress signal about the mean. The system was designed such that the mean stress at the joints during operation is near zero. The fatigue-life curve plots RMS stress level at zero mean against a number of cycles to failure (failure is defined as a crack detectable by visual inspection). Figure B1 shows the results of the test with an estimated mean time to failure curve expressed as a bilinear log-log fit. The slope of the curve at the high cycle end corresponds to  $b = -9.5$  in the equation

$$N(\sigma) = K\sigma^b \quad (\text{B1})$$

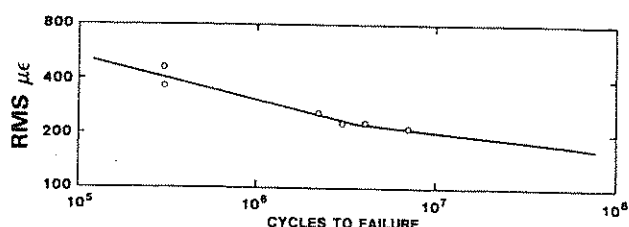


Figure B1. RMS Strain vs Number of Cycles to Failure With a Narrow Band Random Loading for the DOE 100-kW Welded Blade Joint

#### Operating Stress Levels

The turbine at Bushland has strain gages mounted at each joint in the same locations as the strains were monitored in the fatigue tests. The standard deviation of the stress signal during operation was calculated, using a bins type approach as outlined in References 1, 4. Figure B2 is a plot of the measured stress standard deviation as a function of wind speed. One feature of the short averaging time associated with the bins-measuring procedure is that the highest wind-bins estimates are too low and the lowest wind estimates are too high.<sup>5</sup> With this in mind, a linear fit to the data with a slope of  $128 \mu\epsilon/(m/s)$  ( $57 \mu\epsilon/mph$ ) is reasonable.

#### The Maximum Damage Density

By combining the fatigue life curve with the operating stress data, the number of cycles to failure is written directly as a function of wind speed as in Eq (A8). The average cyclic stress frequency can be estimated by taking the ratio of the second moment to the zero moment of the stress frequency spectrum. A typical blade stress spectrum from the DOE 100-kW rotor is shown in Figure B3. The mean crossing rate

calculated from this spectrum is 3.5 Hz, which is higher than might be expected by a visual inspection of the spectrum. As a check on the accuracy of this estimate for use in a fatigue calculation, the number of occurrences of each stress amplitude were counted by the method outlined in Reference 1 using several threshold values for minimum cyclic stress amplitude. The results are shown in Figure B4. As the threshold level is increased, the cyclic stress amplitudes approach the expected Rayleigh distribution. The solid line in Figure B4 is the Rayleigh distribution with a frequency of 3.5 Hz. It is important to note that the mean crossing rate is significantly affected by the high frequency content of the spectrum, even though the high frequency content may appear to be insignificant.

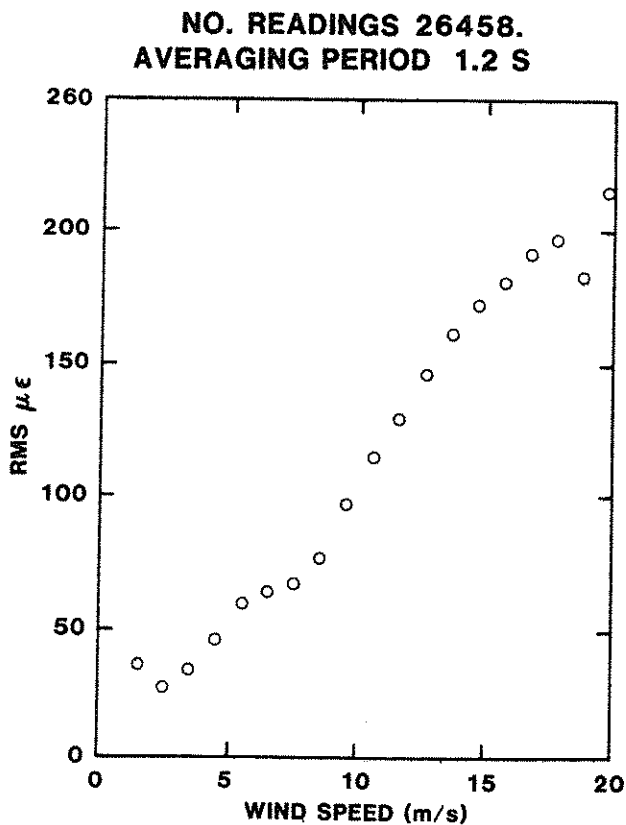


**Figure B2.** Measured RMS Strain vs Wind Speed for the Welded Blade Joint at Bushland, TX

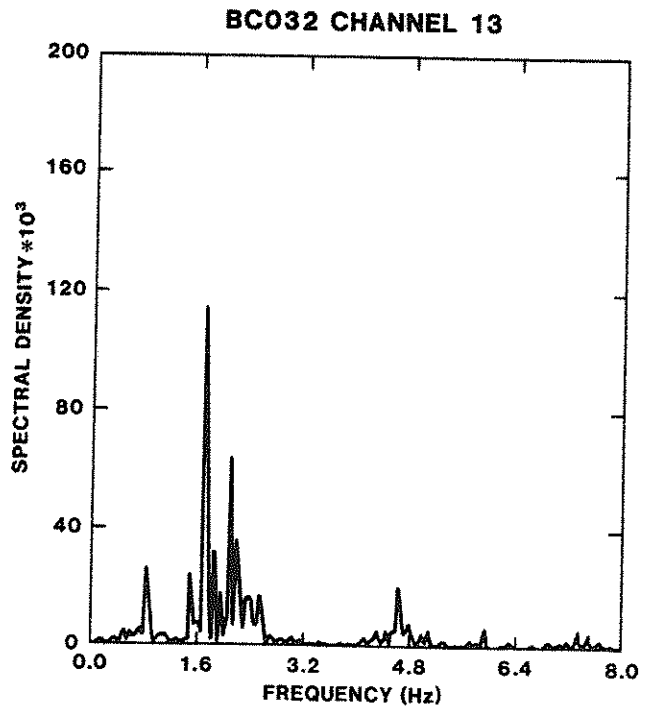


**Figure B3.** DOE 100-kW VAWT Blade Stress Power Spectral Density

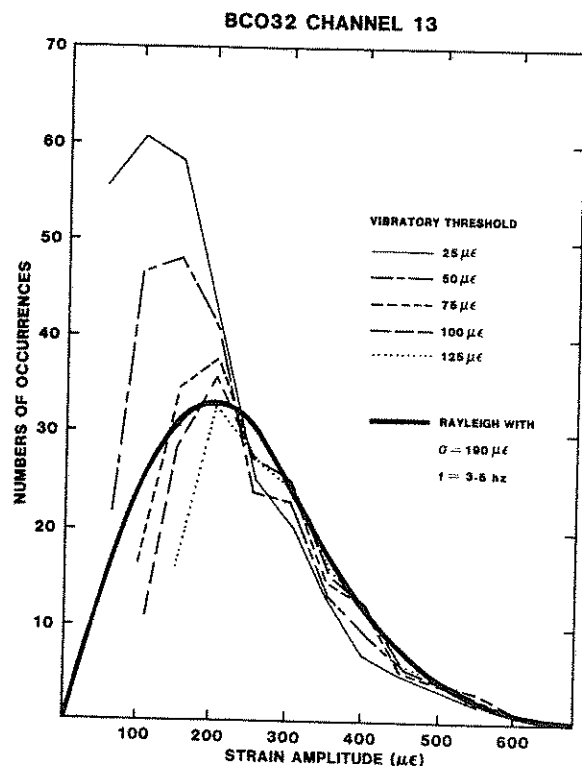


**Figure B4.** Number of Occurrences of each Vibratory Strain Amplitude Level for Several Values of Threshold Strain Amplitude. The heavy line is the theoretical Rayleigh distribution for a record of the same length with identical variance and a frequency of 3.5 Hz.

All the necessary ingredients to evaluate Eq (A11) for the maximum ddf are supplied above. The Rayleigh wind speed distribution from Eq (A3), the number of cycles to failure as a function of wind speed as produced by Eq (A9), and the average cyclic stress frequency are substituted into Eq (A11). This results in a maximum ddf with the functional form

$$d_v(V) = \frac{\pi m^{-b}}{2\bar{V}^2 K} V^{(1-b)} \exp\left(\frac{-\pi V^2}{4\bar{V}^2}\right) \quad (B2)$$

The resulting maximum ddf for the welded joint on the Bushland 100-kW turbine is shown in Figure B5. The time to failure of this component, if the turbine operates at all times, is the inverse of the integral of the maximum ddf: 2.8 yr. The actual life of the joint on a turbine with an active control system can be considerably longer. The increases in joint life expectancy using various cutout wind speeds are included in Table 1.

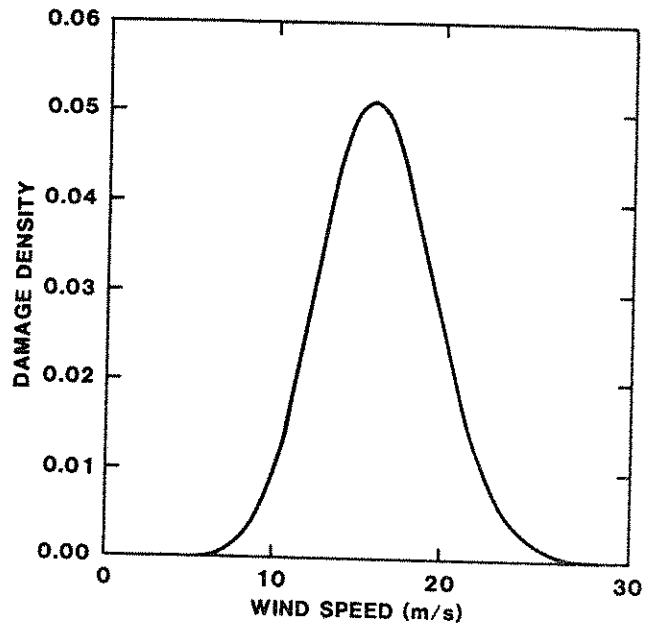


Figure B5. Damage Density Function (ddf) for the Welded Blade Joint of the DOE 100-kW Turbine at Bushland, TX

DISTRIBUTION:

Aeroenvironment, Inc.  
Attn: P. B. S. Lissaman  
660 South Arroyo Parkway  
Pasadena, CA 91105

Aerolite, Inc.  
Attn: R. K. St. Aubin  
550 Russells Mills Road  
South Dartmouth, MA 02748

Alcoa Technical Center (4)  
Aluminum Company of America  
Attn: D. K. Ai  
    J. T. Huang  
    J. R. Jombock  
    J. L. Prohaska  
Alcoa Center, PA 15069

Amarillo College  
Attn: E. Gilmore  
Amarillo, TX 79100

American Wind Energy Association  
1609 Connecticut Ave NW  
Washington, DC 20009

Arizona State University  
University Library  
Attn: M. E. Beecher  
Tempe, AZ 85281

Atlantic Wind Test Site  
PO Box 189  
Attn: R. G. Richards  
Tignish P.E.I.  
CANADA COB 2B0

Battelle-Pacific Northwest Laboratory  
PO Box 999  
Attn: L. Wendell  
Richland, WA 99352

G. Bergeles  
Dept of Mechanical Engineering  
National Technical University  
42, Patission Street  
Athens, GREECE

Bonneville Power Administration  
PO Box 3621  
Attn: N. Butler  
Portland, OR 97225

Burns & Roe, Inc.  
Attn: G. A. Fontana  
800 Kinderkamack Road  
Oradell, NJ 07649

California State Energy Commission  
Research and Development Division  
Attn: J. Lerner  
1111 Howe Ave  
Sacramento, CA 95825

Canadian Standards Association  
Attn: T. Watson  
178 Rexdale Blvd  
Rexdale, Ontario  
CANADA M9W 1R3

V. A. L. Chateau  
School of Engineering  
University of Auckland  
Private Bag  
Auckland, NEW ZEALAND

Colorado State University  
Dept of Civil Engineering  
Attn: R. N. Meroney  
Fort Collins, CO 80521

Commonwealth Electric Co.  
Box 368  
Attn: D. W. Dunham  
Vineyard Haven, MA 02568

Consolidated Edison Company  
4 Irving Place  
Attn: K. Austin  
New York, NY 10003

Cornell University  
Dept of Mechanical and Aerospace Engineering  
Upson Hall  
Attn: G. Wayne  
Ithaca, NY 14853

Curtis Associates  
Attn: G. B. Curtis  
3089 Oro Blanco Drive  
Colorado Springs, CO 80917

M. M. Curvin  
11169 Loop Road  
Soddy Daisy, TN 37379

DISTRIBUTION (cont):

Department of Economic Planning  
and Development  
Barrett Building  
Attn: G. N. Monsson  
Cheyenne, WY 82002

Otto de Vries  
National Aerospace Laboratory  
Anthony Fokkerweg 2  
Amsterdam 1017  
THE NETHERLANDS

DOE/ALO  
Attn: G. P. Tennyson  
Albuquerque, NM 87115

DOE/ALO  
Energy Technology Liaison Office  
NGD  
Attn: J. L. Hanson, USAF  
Albuquerque, NM 87115

DOE Headquarters (20)  
Wind Energy Technology Division  
Attn: L. V. Divone  
P. Goldman  
1000 Independence Ave  
Washington, DC 20585

Dominion Aluminum Fabricating, Ltd. (2)  
Attn: L. Schienbein  
C. Wood  
3570 Hawkestone Road  
Mississauga, Ontario  
CANADA L5C 2V8

J. B. Dragt  
Nederlands Energy Research Foundation  
(E.C.N.)  
Physics Department  
Westerduinweg 3 Patten (nh)  
THE NETHERLANDS

H. M. Drees  
528 Main Street  
Cotuit, MA 02632

Dynergy Systems Corporation  
Attn: C. Fagundes  
821 West L Street  
Los Banos, CA 93635

RANN, Inc.  
Attn: A. J. Eggers, Jr  
Chairman of the Board  
260 Sheridan Ave, Suite 414  
Palo Alto, CA 94306

Electric Power Research Institute (3)  
Attn: E. Demeo  
F. Goodman  
S. Kohan  
3412 Hillview Avenue  
Palo Alto, CA 94304

Alcir de Faro Orlando  
Pontificia Universidade Catolica-PUC/Rj  
Mechanical Engineering Department  
R. Marques de S. Vicente 225  
Rio de Janeiro, BRAZIL

FloWind Corporation (2)  
Attn: S. Tremoulet  
I. E. Vas  
21414 68th Avenue South  
Kent, WA 98031

Forecast Industries, Inc.  
Attn: P. N. Vosburgh  
9733 Coors NW  
Albuquerque, NM 87114

Gates Learjet  
Mid-Continent Airport  
PO Box 7707  
Attn: G. D. Park  
Wichita, KS 67277

H. Gerardin  
Mechanical Engineering Department  
Faculty of Sciences and Engineering  
Universite Laval-Quebec  
CANADA G1K 7P4

R. T. Griffiths  
University College of Swansea  
Dept of Mechanical Engineering  
Singleton Park  
Swansea SA2 8PP  
UNITED KINGDOM

DISTRIBUTION (cont):

Helion, Inc.  
Box 445  
Attn: J. Park, President  
Brownsville, CA 95919

Institut de recherche d'Hydro-Quebec (3)  
Attn: G. Beaulieu  
B. Masse  
I. Paraschivoiu  
1800, Montee Ste-Julie  
Varenes, Quebec  
CANADA JOL 2P0

Iowa State University  
Agricultural Engineering, Room 213  
Attn: L. H. Soderholm  
Ames, IA 50010

JBF Scientific Corporation  
Attn: E. E. Johanson  
2 Jewel Drive  
Wilmington, MA 01887

Kaiser Aluminum and Chemical Sales, Inc.  
Attn: A. A. Hagman  
14200 Cottage Grove Ave  
Dolton, IL 60419

Kaiser Aluminum and Chemical Sales, Inc.  
Attn: D. D. Doerr  
6177 Sunol Blvd  
PO Box 877  
Pleasanton, CA 94566

Kaman Aerospace Corporation  
Attn: W. Batesol  
Old Windsor Road  
Bloomfield, CT 06002

Kansas State University  
Electrical Engineering Department  
Attn: G. L. Johnson  
Manhattan, KS 66506

R. E. Kelland  
The College of Trades and Technology  
PO Box 1693  
Prince Philip Drive  
St. John's, Newfoundland  
CANADA A1C 5P7

KW Control Systems, Inc.  
Attn: R. H. Klein  
RD#4, Box 914C  
South Plank Road  
Middletown, NY 10940

Kalman Nagy Lehoczky  
Cort Adeliers GT. 30  
Oslo 2  
NORWAY

L. Liljidahl  
Building 005, Room 304  
Barc-West  
Beltsville, MD 20705

Olle Ljungstrom  
FFA, The Aeronautical Research Institute  
Box 11021  
S-16111 Bromma  
SWEDEN

Massachusetts Institute  
of Technology (2)  
Attn: N. D. Ham  
W. L. Harris, Aero/Astro Dept  
77 Massachusetts Ave  
Cambridge, MA 02139

H. S. Matsuda  
Composite Materials Laboratory  
Pioneering R&D Laboratories  
Toray Industries, Inc.  
Sonoyama, Otsu, Shiga  
JAPAN 520

Michigan State University  
Division of Engineering Research  
Attn: O. Krauss  
East Lansing, MI 48825

The Mitre Corporation  
Attn: F. R. Eldridge, Jr  
1820 Dolley Madison Blvd  
McLean, VA 22102

Morey/Stjernholm and Associates  
Attn: D. T. Stjernholm  
1050 Magnolia Street  
Colorado Springs, CO 80907

DISTRIBUTION (cont):

Napier College of Commerce  
and Technology  
Tutor Librarian, Technology Faculty  
Colinton Road  
Edinburgh, EH10 5DT  
ENGLAND

NASA Lewis Research Center (2)  
Attn: D. Baldwin  
J. Savino  
21000 Brookpark Road  
Cleveland, OH 44135

National Rural Electric Cooperative Assn  
Attn: W. Prichett III  
1800 Massachusetts Avenue NW  
Washington, DC 20036

Natural Power, Inc.  
Attn: L. Nichols  
New Boston, NH 03070

Northwestern University  
Dept of Civil Engineering  
Attn: R. A. Parmalee  
Evanston, IL 60201

Ohio State University  
Aeronautical and Astronautical Dept  
Attn: G. Gregorek  
2070 Neil Avenue  
Columbus, OH 43210

Oklahoma State University  
Mechanical Engineering Dept  
Attn: D. K. McLaughlin  
Stillwater, OK 76074

Oregon State University (2)  
Mechanical Engineering Dept  
Attn: R. W. Thresher  
R. E. Wilson  
Corvallis, OR 97331

Pacific Gas & Electric  
Attn: T. Hillesland  
3400 Crow Canyon Road  
San Ramon, CA 94583

Troels Friis Pedersen  
Riso National Laboratory  
Postbox 49  
DK-4000 Roskilde  
DENMARK

Helge Petersen  
Riso National Laboratory  
DK-4000 Roskilde  
DENMARK

The Power Company, Inc.  
Attn: A. A. Nedd  
PO Box 221  
Genesee Depot, WI 53217

PRC Energy Analysis Co.  
Attn: E. L. Luther  
7600 Old Springhouse Road  
McLean, VA 22101

Public Service Co. of New Hampshire  
Attn: D. L. C. Frederick  
1000 Elm Street  
Manchester, NH 03105

Public Service Company of New Mexico  
Attn: M. Lechner  
PO Box 2267  
Albuquerque, NM 87103

The Resources Agency  
Department of Water Resources  
Energy Division  
Attn: R. G. Ferreira  
1416 9th Street  
PO Box 388  
Sacramento, CA 95802

Reynolds Metals Company  
Mill Products Division  
Attn: G. E. Lennox  
6601 West Broad Street  
Richmond, VA 23261

A. Robb  
Memorial University of Newfoundland  
Faculty of Engineering and Applied Sciences  
St. John's Newfoundland  
CANADA A1C 5S7

DISTRIBUTION (cont):

Rockwell International (2)  
Rocky Flats Plant  
Attn: T. Healy  
PO Box 464  
Golden, CO 80401

Dr. -Ing. Hans Ruscheweyh  
Institut fur Leichbau  
Technische Hochschule Aachen  
Wullnerstrasse 7  
GERMANY

Beatrice de Saint Louvent  
Etablissement d'Etudes  
et de Recherches  
Meteorologigues  
77, Rue de Serves  
92106 Boulogne-Billancourt Cedex  
FRANCE

National Atomic Museum  
Attn: G. Schreiner  
Librarian  
Albuquerque, NM 87185

Arnan Seginer  
Professor of Aerodynamics  
Technion-Israel Institute of Technology  
Department of Aeronautical Engineering  
Haifa, ISRAEL

Dr. Horst Selzer  
Dipl.-Phys.  
Wehrtechnik und Energieforschung  
ERNO-Raumfahrttechnik GmbH  
Hunefeldstr. 1-5  
Postfach 10 59 09  
2800 Bremen 1  
GERMANY

H. Sevier  
Rocket and Space Division  
Bristol Aerospace Ltd.  
PO Box 874  
Winnipeg, Manitoba  
CANADA R3C 2S4

P. N. Shankar  
Aerodynamics Division  
National Aeronautical Laboratory  
Bangalore 560017  
INDIA

David Sharpe  
Kingston Polytecnic  
Canbury Park Road  
Kingston, Surrey  
UNITED KINGDOM

Kent Smith  
Instituto Technologico Costa Rico  
Apartado 159 Cartago  
COSTA RICA

Solar Initiative  
Citicorp Plaza, Suite 900  
Attn: J. Yudelson  
180 Grand Avenue  
Oakland, CA 94612

Bent Sorenson  
Roskilde University Center  
Energy Group, Bldg 17.2  
IMFUFA  
PO Box 260  
DK-400 Roskilde  
DENMARK

South Dakota School of Mines and Technology  
Dept of Mechanical Engineering  
Attn: E. E. Anderson  
Rapid City, SD 57701

Southern California Edison  
Research & Development Dept, Room 497  
Attn: R. L. Scheffler  
PO Box 800  
Rosemead, CA 91770

Southern Illinois University  
School of Engineering  
Attn: C. W. Dodd  
Carbondale, IL 62901

G. Stacey  
The University of Reading  
Department of Engineering  
Whiteknights, Reading, RG6, 2AY  
ENGLAND

Stanford University  
Dept of Aeronautics and  
Astronautics Mechanical Engineering  
Attn: H. Ashley  
Stanford, CA 94305

DISTRIBUTION (cont):

R. J. Templin (3)  
Low Speed Aerodynamics Section  
NRC-National Aeronautical Establishment  
Ottawa 7, Ontario  
CANADA K1A 0R6

Texas Tech University (2)  
Mechanical Engineering Dept  
Attn: J. W. Oler  
J. Strickland  
PO Box 4389  
Lubbock, TX 79409

Tulane University  
Dept of Mechanical Engineering  
Attn: R. G. Watts  
New Orleans, LA 70018

Tumac Industries, Inc.  
Attn: J. R. McConnell  
650 Ford Street  
Colorado Springs, CO 80915

Air Force Wright Aeronautical  
Laboratories (AFSC)  
Terrestrial Energy Technology Program Office  
Energy Conversion Branch  
Aerospace Power Division  
Aero Propulsion Laboratory  
Attn: J. M. Turner  
Wright-Patterson Air Force Base, OH 45433

University of Alaska  
Geophysical Institute  
Attn: T. Wentink, Jr  
Fairbanks, AK 99701

University of California  
Institute of Geophysics  
and Planetary Physics  
Attn: P. J. Baum  
Riverside, CA 92521

University of Colorado  
Dept of Aerospace Engineering Sciences  
Attn: J. D. Fock, Jr  
Boulder, CO 80309

University of Massachusetts  
Mechanical and Aerospace Engineering Dept  
Attn: D. E. Cromack  
Amherst, MA 01003

University of New Mexico  
New Mexico Engineering Research Institute  
Attn: G. G. Leigh  
Campus PO Box 25  
Albuquerque, NM 87131

University of Oklahoma  
Aero Engineering Department  
Attn: K. Bergey  
Norman, OK 73069

University of Sherbrooke  
Faculty of Applied Science  
Attn: R. Camerero  
Sherbrooke, Quebec  
CANADA J1K 2R1

The University of Tennessee  
Dept of Electrical Engineering  
Attn: T. W. Reddoch  
Knoxville, TN 37916

USDA, Agricultural Research Service  
Southwest Great Plains Research Center  
Attn: R. N. Clark  
Bushland, TX 79012

Utah Power and Light Co.  
Attn: K. R. Rasmussen  
51 East Main Street  
PO Box 277  
American Fork, UT 84003

Washington State University  
Dept of Electrical Engineering  
Attn: F. K. Bechtel  
Pullman, WA 99163

G. R. Watson  
The Energy Center  
Pennine House  
4 Osborne Terrace  
Newcastle upon Tyne NE2 1NE  
UNITED KINGDOM

West Texas State University  
Government Depository Library  
Number 613  
Canyon, TX 79015

DISTRIBUTION (cont):

West Texas State University	1520	D. J. McCloskey
Department of Physics	1523	R. C. Reuter, Jr
Attn: V. Nelson	1523	D. B. Clauss
PO Box 248	1523	D. W. Lobitz
Canyon, TX 79016	1524	P. S. Veers
	1524	W. N. Sullivan
West Virginia University	1600	D. B. Shuster
Dept of Aero Engineering	1630	R. C. Maydew
Attn: R. Walters	1633	R. E. Sheldahl
1062 Kountz Ave	1636	J. K. Cole
Morgantown, WV 26505	1636	D. E. Berg
	2525	R. P. Clark
Central Lincoln People's Utility	3160	J. E. Mitchell (15)
Attn: D. Westlind	3161	P. S. Wilson
2129 North Coast Highway	6000	E. H. Beckner
Newport, OR 97365-1795	6200	V. L. Dugan
	6220	D. G. Schueler
Wichita State University (2)	6225	R. H. Braasch (50)
Aero Engineering Department	6225	R. E. Akins
Attn: M. Snyder	6225	J. D. Cyrus
W. Wentz	6225	R. D. Grover
Wichita, KS 67208	6225	E. G. Kadlec
	6225	P. C. Klimas
Wind Energy Report	6225	M. T. Mattison
Attn: F. S. Seiler	6225	R. O. Nellums
Box 14	6225	M. H. Worstell
102 S Village Avenue	7111	J. W. Reed
Rockville Centre, NY 11571	8424	M. A. Pound
	3141	L. J. Erickson (5)
Wind Power Digest	3151	W. L. Garner (3)
Attn: M. Evans	3154-3	C. H. Dalin (25)
PO Box 700		For DOE/TIC (Unlimited Release)
Bascom, OH 44809		
Wisconsin Division of State Energy		
8th Floor		
Attn: Wind Program Manager		
101 South Webster Street		
Madison, WI 53702		



